Separation of a Density Current from the Bottom of a Continental Slope

MELVIN E. STERN

Department of Oceanography, The Florida State University, Tallahassee, Florida

ABSTRACT

Separation from the continental slope of stratified jets like the Gulf Stream involves the sliding of successive isopycnal layers from a nearly horizontal bottom to the adjacent offshore isopycnal in the deep ocean. One mechanism for producing such an effect is due to a downstream convergence of slope isobaths, as shown herein for a $1\frac{1}{2}$-layer density model. Upstream of the convergence, a geostrophically balanced jet is assumed with an inshore region of cyclonic vorticity resting on the continental slope and an offshore anticyclonic region resting on the isopycnal interface above heavier water. For $O(1)$ Rossby number and cross-stream topographic variation, the steady transverse current displacements forced by slowly varying downstream topography are computed. For "supercritical" upstream flow (i.e., fast compared to free topographic waves) *off* slope displacements are produced by converging isobaths; extrapolation of the small amplitude result suggests that the mechanism is quantitatively important for the explanation of the full separation of the Gulf Stream from the *bottom* of the continental slope. The kinematics involved in this process should apply to a continuously stratified jet, as well as to other forcing mechanisms known to be of importance in continental boundary current separation.

1. Introduction

The Gulf Stream emerging from the Straits of Florida consists of an inshore region with large cyclonic vorticity overlying a steep continental slope, the latter being intersected by isopycnals extending shoreward from the anticyclonic region of the offshore jet. As the stream flows northward (Olsen et al. 1983), there is a continual deflection of successive isopycnal layers off the slope and onto the isopycnals in the deeper ocean. Eventually all of the fluid over the slope separates completely from the *bottom* in a remarkably localized region north of Cape Hatteras, thereby forming a "free" jet in deep water.

Although the separation problem (Haidvogel et al. 1992; Özgökmen et al. 1997) has received considerable attention in the past, the focus has usually been on planetary-scale effects in models whose lateral boundary consisted of a vertical *wall*. One of these effects (with which the separation of the Gulf Stream must be consistent), is the downstream increase in wind-driven transport to higher latitudes, which leads to surfacing of isopycnals near the western wall (Parsons 1969; Morgan 1956; Charney 1955). Other known "global" constraints are associated with the termination of the subtropical gyre at the latitude of vanishing wind stress curl

(Munk 1950), the "collision" of the subtropical gyre with the deep western boundary current (Agra and Nof 1993), and the abrupt change in direction of the coastline (Stern and Whitehead 1990). An indication of the important role of the bottom slope (in contrast to the vertical wall) appears in the barotropic models of Baines and Hughes (1996) and Becker and Salmon (1997). In both of these papers the depth-independent boundary current separates from the slope while remaining in contact with the bottom, whereas our focus will be on the separation of a baroclinic jet from the rigid bottom. Our viewpoint is also more local (f plane), more inertial (larger jet Rossby number), and starts with a specified upstream jet structure with a more realistic inshore (cyclonic) shear. It should be mentioned that there is no accepted explanation for the generation of this shear, as contrasted with the anticyclonic offshore shear.

In connection with Fig. 1, Olsen et al. (1983) mention that "the gradient of bottom topography increases by a factor of 2 around 29°N. At this point the stream leaves the shelf and enters deeper water." More striking is the extreme convergence of the isobaths at 35.5°N; it is at this point, apart from the influence of small amplitude meanders, that the synoptic baroclinic jet separates completely from the continental slope.

We will investigate the topographic effect using a $1\frac{1}{2}$-layer model (Fig. 2) in which the upper layer of uniform density ρ rests partially on the bottom slope and partially on the interface above a stagnant layer of density $\rho + \Delta\rho$; at all cross-stream positions $\hat{y}$ the upstream flow is in geostrophic equilibrium. A steady flow is

Corresponding author address: Dr. Melvin E. Stern, Department of Oceanography (4320), The Florida State University, Tallahassee, FL 32306-4320.
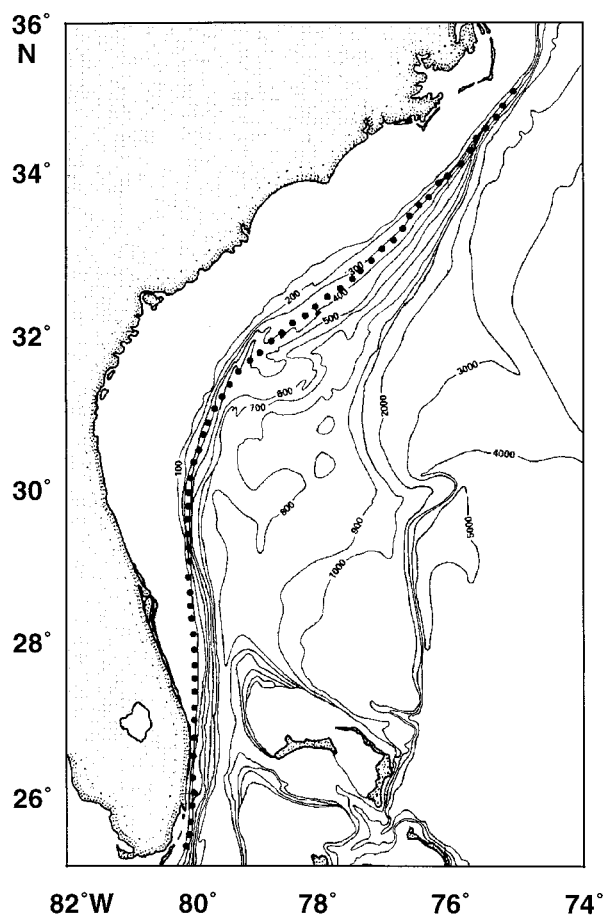E-mail: stern@ocean.fsu.edu

FIG. 1. The path of the mean Gulf Stream (dotted) plotted over the topography of the eastern coast of the United States. After Olsen et al. (1983).

assumed farther downstream where the isobaths converge (or diverge) *gradually* compared to the cross-stream variation. Accordingly, the forced topographic response will be computed by a steady-state long-wave theory, which will eventually be linearized for the case of a small amplitude downstream variation in slope, but neither the cross-stream slope nor the Rossby number will be assumed small in the main calculation (section 4). Also noteworthy (Fig. 2) is the absence of an unrealistic slippery vertical *wall*; instead we have a free streamline with vanishing velocity, located in finite depth water on the bottom slope. This boundary condition and this model are complementary to those in a recent study (Stern 1997) of a free jet flowing over a *sill* with *non*convergent isobaths. Clearly, a combination of both kinds of topography, that is, variation in cross-stream curvature as well as isobath convergence, needs to be considered in general.

The most novel physical consideration (sections 2a–c) in this paper is the connection condition at the point where a material column [a streamline originating at $\hat{y}$ (Fig. 2)] leaves the rigid bottom and moves onto the

density interface; at any downstream section $\hat{\eta}$ ($\hat{y}$) indicates the transverse displacement of any streamline from a designated isobath at $\hat{y} = 0$ (or $\hat{\eta} = 0$). The calculation is eventually limited to small cross-isobath displacements ($\hat{\eta} - \hat{y}$), such as are produced by a small (ε) increase in transverse continental slope at a downstream section ($\hat{x}$) relative to the upstream section.

The aforementioned connection condition provides one boundary condition for the well-known linearized potential vorticity equation (section 2d), which applies to the barotropic fluid on the slope; the second boundary condition requires vanishing velocity on the inshore *free* streamline. The solution of the resulting inhomogeneous ordinary differential equation (section 2) gives the fraction $\delta \hat{y}$ of the upstream current on the slope, which appears downstream on the density interface for a given topographic slope change ε.

For the quasigeostrophic range of topographic, Rossby, and Burger numbers, Eq. (3.3) or Fig. (4) gives an analytic result for $\delta \hat{y}$, and section 4 gives the numerical result for $O(1)$ Rossby number and topographic variation. The extrapolation of this $\delta \hat{y}/\varepsilon$ result, given in the conclusion, provides an order of magnitude estimate of the topographic effect for the Gulf Stream.

2. Derivation of linear equations

Part of the steady upstream jet in Fig. 2 rests on a rigid bottom where the assumed depth and geostrophically balanced velocity are given respectively by

$$H(\hat{y}) = H_0(1 - \hat{y}r/L_0), \qquad U(\hat{y}) = -U_0\hat{y}/L_0,$$

where rH_0/L_0 is the nondimensional slope (assumed constant for $y \geq -L_0$). Farther offshore ($\hat{y} < -L_0$) the geostrophic current lies above a more dense ($\rho + \Delta\rho$) layer, which is assumed to be at rest in the rotating coordinate system with Coriolis parameter f. Going downstream ($\hat{x}$) the bottom depth profile changes to:

$$h(\hat{\eta}) = H_0(1 - \hat{\eta}r(1 + \varepsilon))/L_0,$$

where $\hat{\eta}$ measures the transverse displacement of a material column originating at $\hat{y}$, and ε varies parametrically with x. At any such section the $\hat{\eta} = 0$ origin is taken on the same isobath (H_0) as occurs upstream at $\hat{y} = 0$. Note that the free streamline (Fig. 2) crosses isobaths and is displaced from $\hat{\eta} = 0$ at the downstream end. The parameters in Fig. 2 are assumed to be such that the Lagrangian column originating upstream at $\hat{y} = -L_0$ is deflected *off* the bottom slope and onto the density interface; the dotted curve indicates the intersection of the density interface with the continental slope at any downstream position. Different material columns cross this curve at different downstream positions, causing the transport of the fluid remaining on the slope to decrease. The downstream component of current at all sections is essentially in geostrophic equilibrium (because $\partial/\partial\hat{x}$ is small). The downstream velocities in the boundary current are assumed to vanish at
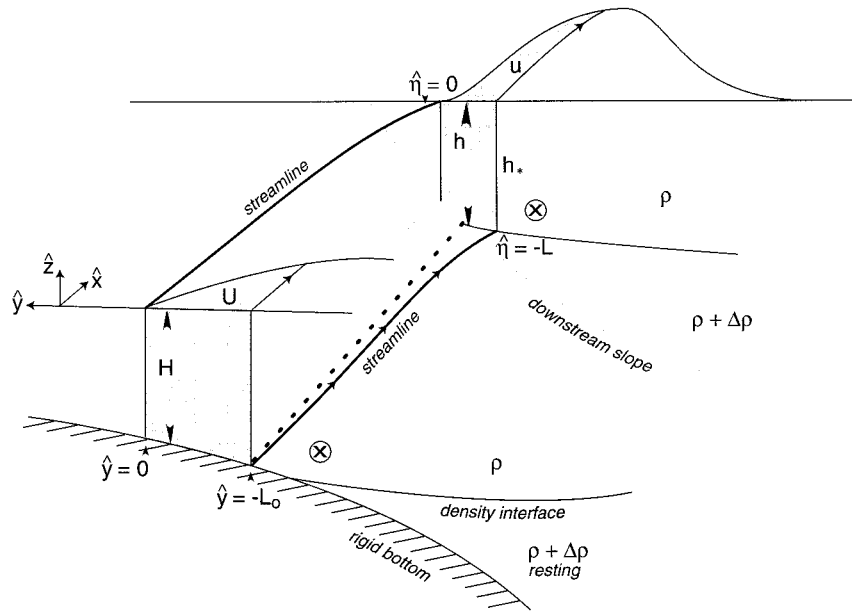
FIG. 2. Perspective sketch of a current separating from a bottom whose slope increases in the downstream direction ($\hat{x}$). The upstream laminar velocity $U(\hat{y})$ is barotropic in $\hat{y} > -L_0$, and at $\hat{y} < -L_0$ the current lies on the density interface of a stagnant layer of resting heavy ($\rho + \Delta\rho$) water. $\hat{\eta}\,(\hat{y})$ is the transverse coordinate of a *material* column originating at $\hat{y}$. As a result of the slow ($\varepsilon \ll 1$) downstream variation of bottom depth [$h(\hat{\eta}) = H_0(1 - \hat{\eta}r(1 + \varepsilon))/L_0)$], columns of fluid are forced offshore at the separation curve (dotted). The $\hat{\eta} = 0$ origin at the downstream end is located on the same isobath as the $\hat{y} = 0$ origin, and $u(\hat{\eta})$, $h(\hat{\eta})$ denote the respective values of downstream current and depth in the long-wave theory. The layer thickness at $\hat{y} = -\infty$ and $\hat{\eta} = -\infty$ are equal.

$\hat{y} = -\infty$ and $\hat{\eta} = -\infty$, and the layer thickness is the same in these two regions.

a. Outer boundary condition for offshore displacement

For gradual changes in bottom slope, a Lagrangian material column ($\hat{y} \geq -L_0$) with downstream velocity $u(\hat{\eta})$, and thickness $h(\hat{\eta})$, satisfies mass conservation in the sense of the long-wave approximation:

$$uh\,d\hat{\eta} = UH\,d\hat{y} = -U_0\hat{y}H\,d\hat{y}/L_0,$$

where $H(\hat{y})$ is the upstream depth of this column. Before applying this to $\hat{y} > -L_0$ and before turning to the potential vorticity equation, we consider the novel boundary condition required at the edge of the barotropic region. First, the previous equation is rewritten as

$$u = -\frac{U_0}{L_0}\frac{H(\hat{y})}{h(\hat{\eta})}\frac{d}{d\hat{\eta}}\frac{\hat{y}^2}{2}$$

$$= -\frac{U_0}{L_0}\frac{H(\hat{y})}{h(\hat{\eta})}\left[\hat{\eta} + L_0\frac{d\hat{\psi}}{d\hat{\eta}} + \frac{L_0^2}{2}\frac{d}{d\hat{\eta}}\frac{\hat{\psi}^2}{\hat{\eta}^2}\right], \quad (2.1a)$$

where the modified Lagrangian displacement function $\hat{\psi}$ is defined by

$$\hat{y} = \hat{\eta} + L_0\hat{\psi}/\hat{\eta}. \quad (2.1b)$$

The geostrophic transport between two streamlines located completely in the deep water is proportional to the square of the difference of the respective layer thickness and, since $H(-\infty) = h(-\infty)$, it follows that the streamline originating at the upstream edge $\hat{y} = -L_0$ of the slope and terminating offshore at $\hat{\eta} = -L$ in the baroclinic region must satisfy $h(-L) = H(-L_0)$. Moreover the Bernoulli invariant on this streamline implies $u(-L) = U_0$. Evaluating (2.1a) and (2.1b) on $\hat{y} = -L_0$ then gives

$$-L_0 = -L + L_0 d\hat{\psi}/d\hat{\eta} + \frac{L_0^2}{2}\left(\frac{d}{d\hat{\eta}}\frac{\hat{\psi}^2}{\hat{\eta}^2}\right)_{\hat{\eta}=-L_0}$$

$$-L_0 = -L - L_0\hat{\psi}/L. \quad (2.1c)$$

Further analysis is now restricted to small ε, in which case $L - L_0$ and $\hat{\psi}$ are correspondingly small. Therefore, when the previous equation is substituted into (2.1c) and the small quadratic terms are neglected, we get a linearized boundary condition:

$$\hat{\psi}(-L_0) + L_0\hat{\psi}'(-L_0) = 0 \quad (2.2)$$

for $\hat{\psi}$ in the barotropic region $\hat{y} > -L_0$. Although the density is not explicitly involved in this relation, its
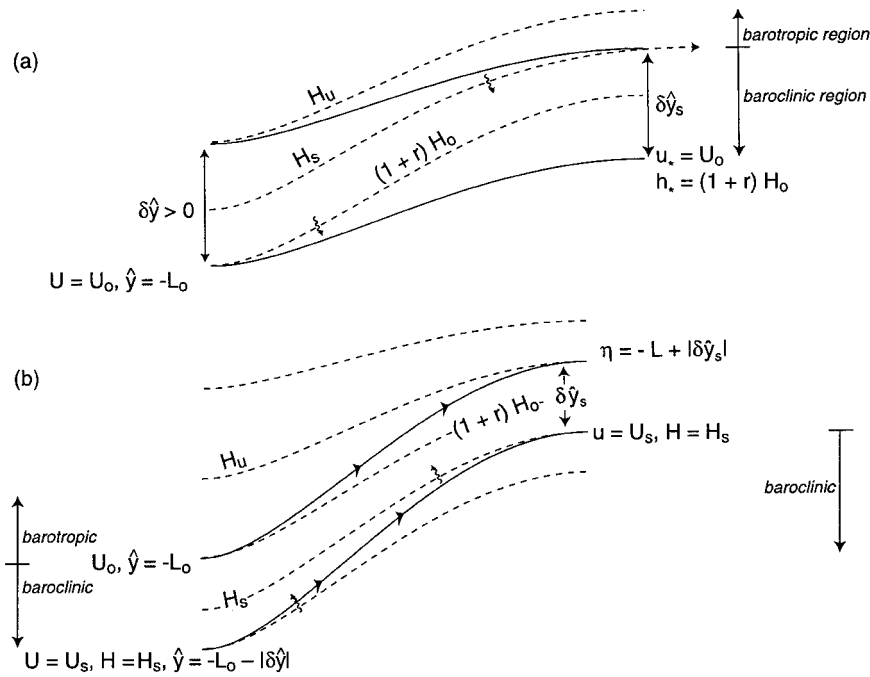
FIG. 3. Plan view of streamlines and isobaths (dashed) near the outer edge of the barotropic region: (a) assuming the streamline originating at $\hat{y} = -L_0$ is deflected offshore and onto the density interface, thereby (see text) conserving its thickness $[(1 + r)H_0]$ and speed (U_0). At the outer edge $\eta = -L + \delta\hat{y}_s$ of the downstream barotropic region the streamline on isobath H_s originates upstream at H_u. The problem is to predict the (small) fraction $\delta\hat{y}$ of the current that separates as a function of ε, and other parameters; (b) assuming the displacement of the $\hat{y} = L_0$ streamline is toward a shallower isobath $H_u < (1 + r)H_0$, which is located at $\eta = -L + |\delta y_s|$. It is shown that for $\varepsilon > 0$ this only occurs for ''subcritical'' velocities relative to the speed of the free topographic waves.

validity clearly depends upon the fact that the outer part of the current originating on the slope lies on the *density* interface. The explicit importance of $\Delta\rho$ will appear subsequently.

The novel Lagrangian function $\hat{\psi}$ in (2.2) will now be related to the conventional Eulerian mass transport function M defined by

$$v_1 = H^{-1}(\hat{y})\frac{\partial M}{\partial\hat{x}}, \qquad u_1 = -H^{-1}\frac{\partial M}{\partial\hat{y}}, \quad (2.3)$$

where (v_1, u_1) are the cross-stream and downstream $(\hat{x})$ perturbation velocities, respectively. [N.B., no confusion should arise here or in section 2d by the use of $\hat{y}$ as transverse Eulerian coordinate for $M(\hat{x}, \hat{y})$]. On a steady Lagrangian streamline, transversely displaced by an amount $\hat{\eta} - \hat{y}$, we also have $v_1 = U(\hat{y})\partial(\hat{\eta} - \hat{y})/\partial(\hat{x})$, and the linearization of Eq. (2.1b) gives:

$$v_1 = -U(\hat{y})\frac{L_0}{\hat{\eta}}\frac{\partial}{\partial\hat{x}}\hat{\psi} \approx U_0\frac{\partial\hat{\psi}}{\partial\hat{x}},$$

where $\hat{\eta} \approx \hat{y}$, and $U(\hat{y}) = -U_0\hat{y}/L_0$ have been used. The first equation in (2.3) then integrates to:

$$\hat{\psi}(\hat{y}) = \frac{M(\hat{y})}{U_0 H(\hat{y})}, \qquad (2.4)$$

and by substituting this in (2.2) we get

$$\alpha M(-L_0) + L_0 M'(-L_0) = 0 \qquad (2.5)$$

$$\alpha \equiv 1 - \frac{L_0 H'(-L_0)}{H(-L_0)} = 1 + \frac{r}{1 + r}. \qquad (2.6)$$

Equation (2.5) provides a boundary condition for the $M(\hat{y})$ satisfying the linearized Eulerian potential vorticity equation appearing in section 2d.

b. The offshore transport relation

The main calculation pertains to the fraction $\delta\hat{y} > 0$ (Fig. 3a) of the upstream slope current, which separates from the bottom and which appears on the density interface in an interval $\delta\hat{y}_s$. At the outermost limit ($\hat{\eta} = -L$) of this interval, the layer thickness h_* and the velocity u_* must equal the corresponding upstream values on the $(1 + r)H_0$ isobath (for ''transport'' and ''Ber-

noulli'' reasons previously mentioned). Correct to first order, the conservation of mass in the intervals then requires

$$\delta\hat{y} = \delta\hat{y}_s. \qquad (2.7)$$

This will be computed by relating it, as follows, to the vorticity perturbation in the barotropic region, and the latter quantity will be related to ε in the Eulerian calculations of section 2d.

If H_s denotes the isobath (Fig. 3a) of the streamline at the *inner* edge of the baroclinic region $-L + \delta\hat{y}_s$, then the integrals of the geostrophic balance equation across the $\delta\hat{y}_s = \delta\hat{y}$ intervals yield

$$fU_0\delta\hat{y} = g^*[(1 + r)H_0 - H_s],$$
$$g^* = g\Delta\rho/\rho. \qquad (2.8)$$

The aforementioned streamline originating at $\hat{y} = -L_0 + \delta\hat{y}$, where $H(\hat{y}) \equiv H_u$, and conserving potential vorticity, increases its relative vorticity at $\hat{\eta} = -L + \delta\hat{y}_s$ by the amount

$$\zeta(-L) = \frac{H_s - H_u}{H_u}(f + \overline{\zeta}), \qquad (2.8a)$$

where the basic upstream vorticity is

$$\overline{\zeta} = U_0/L_0.$$

Equation (2.8a) is the vorticity perturbation along a *streamline,* but because the cross-stream gradient of *undisturbed* vorticity vanishes, Eq. (2.8a) also equals (to leading order) the *perturbation* vorticity along a line that is at equal transverse distances from the H_0 reference isobath at all downstream distances $\hat{x}$.

When (2.8a) is used to eliminate H_s, Eq. (2.8) becomes

$$\frac{(1 + r)H_0 - H_u - \frac{fU_0}{g^*}\delta\hat{y}}{H_u} = \frac{\zeta}{f + \overline{\zeta}},$$

and then the geometrical relation $(1 + r)H_0 - H_u = H_0 r\delta\hat{y}/L_0$ yields

$$\frac{\delta\hat{y}}{L_0} = \frac{\zeta(-L_0)}{f + \overline{\zeta}}\left(\frac{r}{1 + r} - \frac{\overline{\zeta}}{f}F^2\right)^{-1}, \qquad (2.9)$$

where

$$F^2 = \frac{f^2L_0^2}{g^*H_u} \approx \frac{f^2L_0^2}{g^*H_0(1 + r)}. \qquad (2.10)$$

and F is the inverse ratio of the radius of deformation divided by L_0. The perturbation vorticity $\zeta(-L_0)$ computed in sections 3 and 4 will be substituted in (2.9) to obtain the fraction of the fluid deflected offshore for any ε.

It is important to note that the slope $-dH/d\hat{y} = H_0 r/L_0$ of the bottom (Fig. 2) must exceed the slope (S) of the intersecting interface at $\hat{y} = -L_0$, as given geostrophically by

$$S = fU_0/g^*, \qquad (2.11a)$$

and this requires

$$r > \frac{\overline{\zeta}F^2}{f}(1 + r). \qquad (2.11b)$$

Since $\delta\hat{y} > 0$ has been assumed here, Eq. (2.9) requires that the sign of ε be such that $\zeta(-L_0) > 0$.

c. Onshore deflection (Fig. 3b)

Although this case is not considered further here, it is of interest to derive the connection condition when the parameters are such that the streamline at $\hat{y} = -L_0$ is deflected toward the shallower H_u isobath located at $\hat{\eta} = -L + |\delta\hat{y}_s|$, while the outermost barotropic streamline (at $\hat{\eta} = -L$) originates offshore at $\hat{y} = -L_0 - |\delta\hat{y}|$, where $U_s > U_0$ and $H_s > H_u$. As before, mass conservation requires $uh\,d\hat{\eta} = UH\,d\hat{y}$. If the linear part of the upstream shear flow $U(\hat{y})$ extends somewhat beyond $\hat{y} = -L_0$, then $U(\hat{y}) = U_s\hat{y}(-L_0 - |\delta\hat{y}|)^{-1}$, where $U_s = U_0(L_0 + |\delta\hat{y}|)L_0^{-1}$. With the definition $\hat{y} \equiv \hat{\eta} + L_0\hat{\psi}/\hat{\eta}$, it follows that

$$u = \frac{U_s}{(-L_0 - |\delta\hat{y}|)}\frac{H(\hat{y})}{h(\hat{\eta})}\frac{d}{d\eta}\frac{(\hat{\eta} + L_0\hat{\psi}/\hat{\eta})^2}{2}.$$

At $\eta = -L$, $u = U_s$, $H = h$, and linearization yields

$$-L_0 - |\delta\hat{y}| = -L + L_0\,d\hat{\psi}/d\hat{\eta} + O(\psi^2).$$

Since $-L_0 - |\delta\hat{y}| \approx -L - \hat{\psi}$ follows from the definition of $\hat{\psi}$, it is now apparent that (2.2) also applies to this case, and likewise for (2.6).

It only remains to show that (2.9)–(2.10) also applies, provided $\delta\hat{y}$ is replaced by $|\delta\hat{y}|$. The geostrophic velocity integral across the upstream baroclinic $|\delta\hat{y}|$ interval is

$$fU_0|\delta\hat{y}| = g^*[H_s - (1 + r)H_0],$$

and, when the downstream geometrical relation

$$H_s - H_u = |\delta\hat{y}_s|\frac{H_0}{L}r(1 + \varepsilon) \cong \frac{|\delta\hat{y}|}{L_0}H_0 r$$

is used, the result is

$$\frac{fU_0}{g^*}|\delta\hat{y}| \approx H_u - (1 + r)H_0 + \frac{|\delta\hat{y}|H_0 r}{L_0}.$$

From the conservation of potential vorticity at $\eta = -L + |\delta\hat{y}_s|$ we obtain the relative vorticity

$$\zeta = \frac{(f + \overline{\zeta})[H_u - (1 + r)H_0]}{(1 + r)H_0} < 0,$$

and then the proceeding equation becomes

$$\frac{|\delta\hat{y}|}{L_0} = \frac{-\zeta(-L_0)}{f + \overline{\zeta}}\left(\frac{r}{1 + r} - \frac{F^2\overline{\zeta}}{f}\right)^{-1},$$

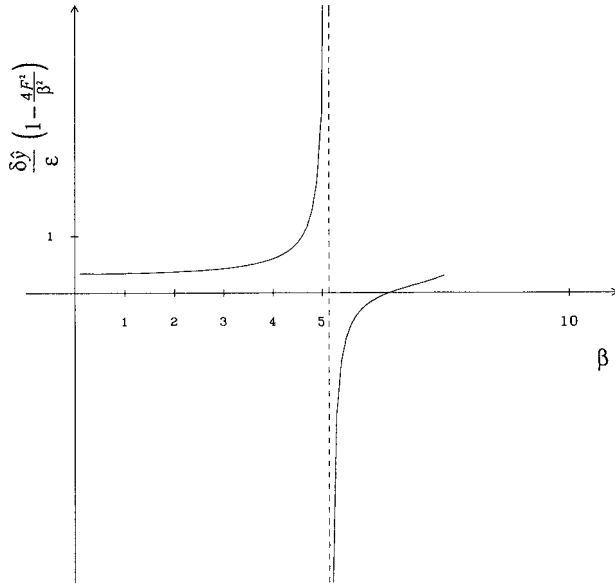which is the same as (2.9) except that the perturbation vorticity must be negative for this case.

FIG. 4. Plot of $8/\beta^2 - 2J_1(\beta)/J_2(\beta)$ as a function of $\beta = 2(r/\zeta_*)^{1/2}$, giving the fractional offshore displacement $\delta\hat{y}/\varepsilon$ in the quasigeostrophic limit [Eq. (3.3)]. Stationary wave resonance occurs for $\beta = 5.1$, and Fig. 5 gives the condition when ζ_* and r are $O(1)$.

d. Barotropic perturbation equation for slow downstream variation

In the following consideration of the Eulerian perturbation equations at any downstream section $(\hat{x})$, the symbol for the previously used Lagrangian coordinate $(\hat{\eta})$ will be replaced by $\hat{y}$, this being the transverse distance from the local isobath $H(0) = H_0$. With this understanding we may write $H_0[1 - r\hat{y}(1 + \varepsilon)]$ for the depth at the downstream section, while retaining $H(\hat{y}) = H_0[1 - r\hat{y}]$ for the upstream depth profile. Thus the potential vorticity at the downstream end is expanded as

$$\frac{f + \overline{\zeta} + \zeta}{H(\hat{y}) - \dfrac{\hat{y}rH_0\varepsilon}{L_0}} = \frac{f + \overline{\zeta} + \zeta}{H(\hat{y})}\left[1 + \frac{\hat{y}rH_0\varepsilon}{HL_0} + \cdots\right],$$

and the linearized Eulerian steady-state conservation equation is

$$U(\hat{y})\frac{\partial\zeta}{\partial\hat{x}} + v_1 H\frac{\partial}{\partial\hat{y}}\frac{f + \overline{\zeta}}{H(\hat{y})} + \frac{f + \overline{\zeta}}{H}\frac{r\hat{y}H_0}{L_0}U\frac{\partial\varepsilon}{\partial\hat{x}} = 0.$$

By using (2.3) and the long-wave approximation $(\partial v_1/\partial\hat{x} \ll \partial u_1/\partial\hat{y})$ the perturbation vorticity becomes

$$\zeta = \frac{\partial}{\partial\hat{y}}\frac{1}{H}\frac{\partial M}{\partial\hat{y}}, \tag{2.12}$$

and thus the previous equation can then be integrated in $\hat{x}$ to give

$$\frac{d}{d\hat{y}}\frac{1}{1 - \hat{y}r/L_0}\frac{dM}{d\hat{y}} + \frac{M(f + \overline{\zeta})}{U(\hat{y})}\frac{d}{d\hat{y}}\frac{1}{1 - \hat{y}r/L_0}$$
$$= -\frac{(f + \overline{\zeta})}{1 - \hat{y}r/L_0}\frac{r\hat{y}H_0\varepsilon(x)}{L_0}.$$

When this is nondimensionalized using

$$\hat{y} = -yL_0, \qquad M(\hat{y}) = \overline{\varepsilon}\,\psi(y), \qquad \zeta_* = \overline{\zeta}/f,$$

$$\delta y = +\delta\hat{y}/L_0, \qquad U = f\zeta_*L_0y,$$

$$\overline{\varepsilon} = \varepsilon fr(1 + \zeta_*)L_0^2 H_0, \tag{2.13}$$

it becomes

$$\frac{d}{dy}\frac{1}{1 + yr}\frac{d\psi}{dy} + \frac{r(1 + \zeta_*)}{\zeta_*}\frac{\psi}{y(1 + ry)^2} = \frac{y}{1 + yr}, \tag{2.14}$$

and the boundary condition (2.5) becomes

$$\psi'(1) - \alpha\psi(1) = 0. \tag{2.15a}$$

(Note that this streamfunction is not the same as the $\hat{\psi}$ used in section 2a.) On the free streamline, with unknown but *small y* ordinate both velocity components vanish, and therefore to leading order, we require $v(0) = 0$, $M(0) = 0$, and therefore

$$\psi(0) = 0. \tag{2.15b}$$

This boundary condition will provide the only solution of (2.14), which is regular near $y = 0$. The quantity of interest for Eq. (2.9) is

$$\frac{\zeta(-L_0)}{f} = \varepsilon r(1 + \zeta_*)\left[\frac{d}{dy}\frac{1}{1 + ry}\frac{d\psi}{dy}\right]_{y=1}$$

$$= \frac{\varepsilon r(1 + \zeta_*)}{1 + r}\left[1 - \frac{r}{1 + r}\frac{(1 + \zeta_*)}{\zeta_*}\psi(1)\right],$$

and therefore (2.9) can be written as

$$\frac{\delta\hat{y}}{\varepsilon} = (1 + r)^{-1}\left(\frac{1}{1 + r} - \frac{\zeta_* F^2}{r}\right)^{-1}$$

$$\times\left[1 - \left(\frac{r}{\zeta_*}\right)(1 + \zeta_*)(1 + r)^{-1}\psi(1)\right]. \tag{2.16}$$

Instead of considering the inhomogeneous equation (2.14), a simplification can be achieved in terms of a solution $\psi_0(y)$ of the homogeneous equation

$$\frac{d}{dy}\frac{1}{1 + ry}\frac{d\psi_0}{dy} + \frac{r(1 + \zeta_*)}{\zeta_*}\frac{\psi_0}{y(1 + ry)^2} = 0, \tag{2.17}$$

which satisfies

$$\psi_0(0) = 0.$$

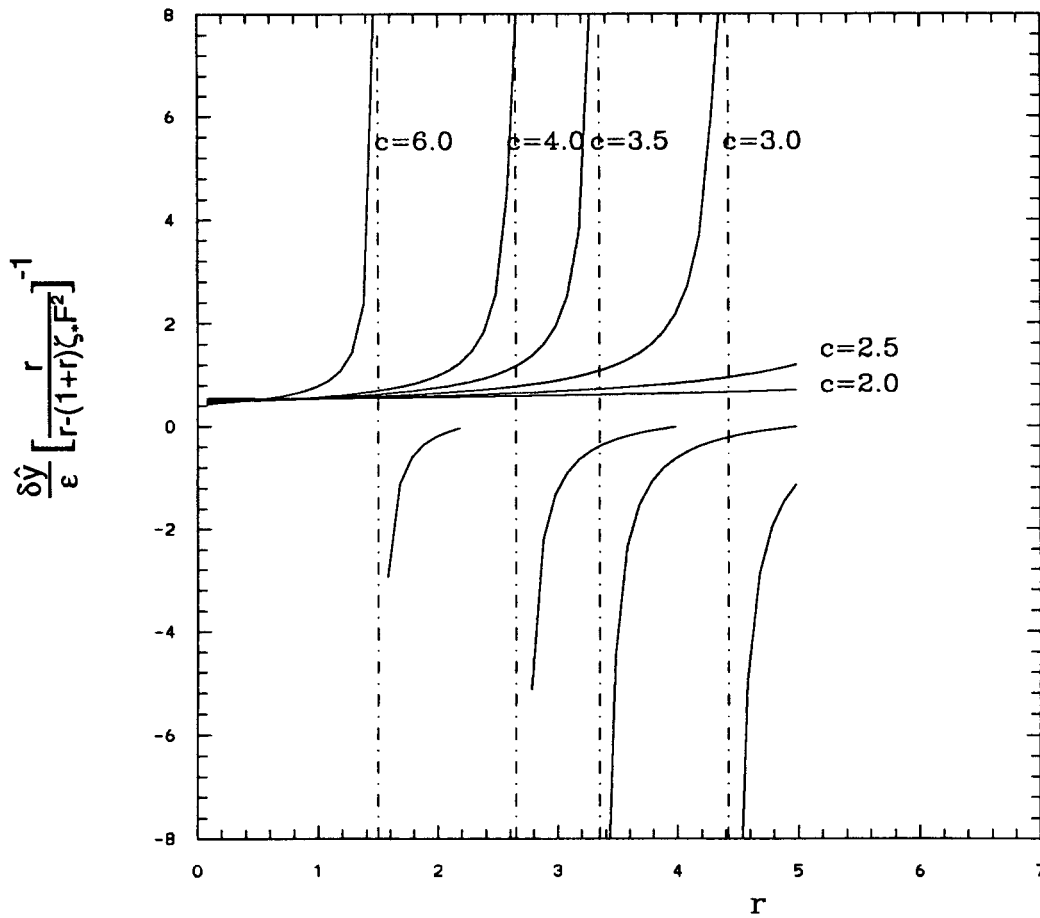Now multiply Eq. (2.17) by $\psi(y)$, multiply Eq. (2.14) by ψ_0, subtract the results, and then integrate to get

FIG. 5. Plot of Eq. (4.4) as a function of slope (r) and c [Eq. (4.1)] for various Burger numbers (2.10). The dashed vertical lines give the values of a downstream uniform r for which a stationary free wave occurs. On the smaller side of each critical r the flow is subcritical, and for $\varepsilon > 0$ the positive δy corresponds to separation (Figs. 2, 3a). For c = 2.0 the value of the ordinate at $r = 0.1$ is 0.548, and this value of $1 + G(r, c)$ may be used over a much wider range of (r, c).

$$\frac{\psi_0(1)\psi'(1) - \psi(1)\psi_0'(1)}{1 + r} = \int_0^1 dy \frac{y\psi_0(y)}{1 + yr}.$$

When the boundary condition (2.15a) for $\psi'(1)$ is applied this becomes:

$$\psi(1) = \frac{1 + r}{\alpha\psi_0(1) - \psi_0'(1)} \int_0^1 dy \frac{y\psi_0(y)}{1 + yr},$$

and thus the final expression of (2.16), or

$$\frac{\delta\hat{y}}{\varepsilon} = \frac{r}{(1 + r)\left(\dfrac{r}{1 + r} - \zeta_*F^2\right)}$$

$$\times \left[1 + \frac{r(1 + \zeta_*)/\zeta_*}{\psi_0'(1) - \alpha\psi_0(1)} \int_0^1 dy \frac{y\psi_0(y)}{1 + ry}\right], \quad (2.18)$$

only requires the solution of (2.17).

3. The quasigeostrophic limit $r = 0(\zeta_*) \to 0$

Before proceeding to the relevant Gulf Stream case, where both the Rossby number ζ_* and r are $O(1)$, it is instructive to consider the quasigeostrophic limit for which analytical results are obtainable. In the latter case r and ζ_* are both small to the same order, and Eqs. (2.14), (2.15), (2.17) reduce to

$$\frac{d^2\psi}{dy^2} + \frac{\beta^2}{4y}\psi = y,$$

$$\psi'(1) - \psi(1) = 0$$

$$\psi(0) = 0$$

$$\frac{\beta^2}{4} \equiv \frac{r}{\zeta_*} = O(1). \quad (3.1)$$

Direct substitution reveals that a particular solution of

(3.1) is $(y^2 - 8y/\beta^2)(4/\beta^2)$, and the only regular homogeneous solution (Abromowitz and Stegun 1970) is $Ay^{1/2}J_1(\beta y^{1/2})$, where J_1 is the first-order Bessel function and A is an amplitude factor. Thus,

$$\psi = Ay^{1/2}J_1(\beta y^{1/2}) + \frac{4y^2}{\beta^2} - \frac{32y}{\beta^4},$$

and the $y = 1$ boundary condition is satisfied if

$$0 = A\left[\frac{1}{2}J_1(\beta) + \frac{\beta}{2}J_1'(\beta) - J_1/\beta)\right] + \frac{4}{\beta^2},$$

or

$$A = \frac{8}{\beta^3 J_2(\beta)}.$$

Thus the complete solution for the quasigeostrophic streamfunction is

$$\psi = \frac{8y^{1/2}J_1(\beta y^{1/2})}{\beta^3 J_2(\beta)} + \frac{4y^2}{\beta^2} - \frac{32y}{\beta^4}. \qquad (3.2)$$

The $r \to 0$, $\zeta_* \to 0$ limit of (2.16) is

$$\frac{\delta\hat{y}}{\varepsilon} = (1 - 4F^2/\beta^2)^{-1}(1 - \beta^2\psi(1)/4),$$

and, when (3.2) is used, we get the explicit result

$$\frac{\delta\hat{y}}{\varepsilon} = (1 - 4F^2/\beta^2)^{-1}\left(\frac{8}{\beta^2} - \frac{2J_1(\beta)}{\beta J_2(\beta)}\right), \qquad (3.3)$$

wherein Eq. (2.11b) requires $4F^2/\beta^2 < 1$. Equation (3.3), plotted in Fig. 4, shows that the deflection into deep water ($\delta\hat{y} > 0$) occurs when $\beta = 2(r/\zeta_*)^{1/2}$ is less than $\beta = 5.1$ [i.e., $J_2(\beta) = 0$], at which value *resonance* occurs. We note in passing that there are free ($\varepsilon = 0$) stationary waves at these values of $J_2(\beta) = 0$, and for such conditions at a point on the continental slope an upstream–downstream hydraulic transition (Hughes 1986) could occur. For $\beta < 5.1$ the flow is said to be supercritical ("fast") with respect to the topographic wave speed, and we conclude that such a flow will produce displacements into deeper water if the isobaths converge downstream.

A final qualitative point may be noted before turning to larger ζ_*, and r. Using Eq. (3.2), we see that the vorticity perturbation, as given by the first term in (3.1) or by $y - (\beta^2/4y)\psi(y)$, has a value near $y = 0$ equal to

$$y - \frac{\beta^2}{4}\left[\frac{4y}{\beta^2} - \frac{32}{\beta^4} + \frac{4}{\beta^2 J_2(\beta)}\right] + O(y^2)$$

$$= \frac{8}{\beta^2} - \frac{1}{J_2(\beta)} = \frac{8}{\beta^2} - \frac{1}{\left(\dfrac{\beta^2}{8} - \cdots\right)} < 0,$$

which is *negative* for β smaller than the first zero of $J_2(\beta) = 0$ since the expansion of $J_2(\beta) = \beta^2/8 - \cdots$ is *less* than $\beta^2/8$. Thus we conclude that for supercritical flow the vorticity at $y = 0$ is *negative* so that here the streamlines are deflected into *shallower* water and its shear decreases (while the velocity remains zero). Near $y = 1$, on the other hand, the vorticity is proportional to $1 - \beta^2/4\psi(1)$, and the discussion following (3.3) shows that this is *positive*. Although the streamlines near $y = 1$ are deflected toward the H_0 isobath, the *isobaths* near $y = 1$ are displaced by a larger amount, and this explains why the $y = 1$ streamline crosses its upstream isobath and emerges into deeper water (where its vorticity increases).

4. Numerical calculations for finite r, ζ_*

With the transformation

$$z = ry, \qquad \psi_0(y) = \phi(z), \qquad (1 + \zeta_*)/\zeta_* = c, \quad (4.1)$$

Eq. (2.17) becomes

$$(1 + z)\frac{d^2\phi}{dz^2} - \frac{d\phi}{dz} + \frac{c}{z}\phi = 0, \qquad (4.2)$$

and (2.18) becomes

$$\frac{\delta\hat{y}}{\varepsilon}\left[\frac{r}{r - (1 + r)\zeta_* F^2}\right]^{-1} = 1 + G(r, c), \quad (4.3)$$

where

$$G(r, z) \equiv \frac{c}{r[r\phi'(r) - \alpha\phi(r)]}\int_0^r \frac{dz\, z\phi(z)}{1 + z}. \quad (4.4)$$

The evaluation of this requires a calculation of $\phi(z)$ up to $z = r$.

For $r < 1$, Eq. (4.4) can be computed by means of a power series solution of (4.2) in the interval of convergence $|z| < 1$, and the result is

$$\phi = \sum_1^\infty a_J z^J$$

$$a_1 = 1, \qquad a_2 = -(c - 1)/2$$

$$a_{J+2} = -a_{J+1}\left[\frac{J^2 - 1 + c}{(J + 2)(J + 1)}\right].$$

In order to obtain solution for $r > 1$, this power series was first used to compute $\phi(z)$ at $z = 0.5$, and then the values of $\phi(0.5)$, $\phi'(0.5)$ were used in a second-order Runge-Kutta integration to continue the solution to $z > 1$ and $r > 1$. The resulting values of $1 + G$, or Eq. (4.3), are plotted in Fig. 5.

For $r \to 0$ and $z \to 0$ the asymptotic value of (4.4), as obtained from

$$r[r\phi'(r) - \phi(r) - r(1 + r)^{-1}\phi(r)]$$
$$= r^3[2a_2 - a_2 - 1] + \cdots = -r^3(c + 1)/2 + \cdots$$

and

$$\int_0^r \frac{dz\, z\phi(z)}{1 + z} = \frac{r^3}{3} + \cdots$$

is

$$1 + G(r, c) = 1 - \frac{2c}{3(c + 1)} + \cdots. \qquad (4.5)$$

For $\zeta_* = 1$, $c = 2$ the value of (4.5) is $1 + G = 5/9$, and this not only agrees with the numerical calculation (Fig. 5) for $r \to 0$, but is a *fair approximation* up to $r = 5.0$ where $1 + G = 0.69$. The most noteworthy numerical variation in $1 + G$ [or Eq. (4.4)] at smaller ζ_* (larger c) is the appearance of a resonance amplification due to the decrease of the current relative to the topographic slope r; this allows stationary topographic Rossby waves in the basic state. It is also clear that for certain values, for example, $r = 2$, $c = 6$, an *onshore* deflection occurs even for convergent isobaths ($\varepsilon > 0$). This is unlikely to occur, however, if the inshore shear is less than $\bar{\zeta} = f/2$ ($c = 3$). If the isobaths are divergent ($\varepsilon < 0$) and $\bar{\zeta} = 0.2f$ ($c = 6.0$), then an *onshore* deflection occurs for $r < 1.5$.

5. Conclusions

The separation of a baroclinic boundary jet from the continental slope requires fluid in contact with the nearly horizontal rigid bottom to be displaced onto an isopycnal surface in the deep ocean. The geostrophic kinematics (Figs. 2 and 3) involved in this process have been applied to a topographic forcing mechanism acting on a "fast" (supercritical) boundary jet. It has been shown that isobaths converging downstream ($\varepsilon > 0$) produce offshore deflection of the slope current at a rate ($\delta\hat{y}/\varepsilon$) given analytically by Eq. (3.3) for a quasigeostrophic jet, and by Fig. 5 when r and ζ are $O(1)$, as is the case for the Gulf Stream. Onshore deflection for convergent isobaths occurs when the jet is subcritical (cf. Fig. 5, lower curves). Conditions for stationary waves, indicative of hydraulic control, have also been given for a jet with a free streamline on a uniformly sloping continental boundary.

The foregoing results may be used to estimate the magnitude of the effect on the Gulf Stream. If $dr/d\hat{x}$, $dL/d\hat{x}$ denote the respective change in slope and width of the overlying current per unit downstream distance ($\hat{x}$), then

$$-\frac{L^{-1}dL/d\hat{x}}{r^{-1}dr/d\hat{x}} = \frac{\delta\hat{y}}{\varepsilon}$$

is given by Eq. (4.3). Since the typical nondimensional Gulf Stream cyclonic vorticity lies between $\zeta_* = 0.5$ and 1.0, the asymptotic limit

$$1 + G(r, c) \approx 5/9$$

is an acceptable approximation for Eq. (4.3), as indicated at the end of section 4. From $\zeta_* = U_0/(fL_0)$, (2.10), and (2.11a), we have

$$\zeta_* F^2 = \frac{L_0 S}{H_0(1 + r)},$$

and therefore Eq. (4.3) then gives

$$-\frac{L^{-1}dL/dx}{r^{-1}dr/dx} \approx \frac{(5/9)r}{(L_0/H_0)} \frac{1}{[-dH/d\hat{y} - S]}$$
$$= \frac{(5/9)(-dH/d\hat{y})}{[-dH/d\hat{y} - S]}.$$

As previously mentioned $S/(-dH/d\hat{y})$ is less than unity, and for order of magnitude purposes we now assume that the ratio is 0.5, in which case

$$\frac{-L^{-1}dL/d\hat{x}}{r^{-1}dr/d\hat{x}} \cong \frac{5/9}{0.5} \approx 1.$$

Thus the width L of the current on the slope decreases by 50% if the cross-stream slope (r) increases by a factor of 2 from the upstream to the downstream section.

This suggests that the geographical *localization* of the *synoptic* Gulf Stream separation point frequently observed at Cape Hatteras is due to the extreme convergence of the slope isobaths at this point. This does not preclude an important role for the other mechanisms cited in the introduction, but these provide "large"-scale and necessary climatalogical conditions in which the inertial–synoptic separation event occurs. Although the foregoing numerical conclusion is based on an extrapolation of small amplitude theory and is applied to simplified baroclinic current (Fig. 2), this model contains important and realistic physical features not found in previous theories; these features include a full jet with both cyclonic and anticyclonic shear and with a free streamline overlying a sloping *bottom* from which separation occurs. The explicit demonstration of the way in which particles separate from a rigid bottom is perhaps the most important fluid dynamical result.

REFERENCES

Abromowitz, M., and A. Stegun, 1970: *Handbook of Mathematical Functions.* Dover, 1043 pp.

Agra, C., and D. Nof, 1993: Collision and separation of boundary currents. *Deep-Sea Res.,* **40,** 2259–2282.

Baines, P. G., and R. L. Hughes, 1996: Western boundary current separation: Inferences from a laboratory experiment. *J. Phys. Oceanogr.,* **26,** 2576–2588.

Becker, J. M., and R. Salmon, 1997: Eddy formation on a continental slope. *J. Mar. Res.,* **55,** 181–200.

Charney, J. G., 1955: The Gulf Steam as an inertial boundary layer. *Proc. Natl. Acad. Sci.,* **41,** 731–740.

Haidvogel, D. B., J. C. McWilliams, and P. R. Gent, 1992: Boundary current separation in a quasi-geostrophic eddy resolving ocean circulation. *J. Phys. Oceanogr.,* **22,** 882–902.

Hughes, R. L., 1986: On the role of criticality in coastal flows over irregular topography. *Dyn. Atmos. Oceans.,* **10,** 129–147.

Morgan, G. W., 1956: On the wind-driven circulation. *Tellus,* **8,** 301–320.

Munk, W. H., 1950: On the wind-driven ocean circulation. *J. Meteor.,* **7,** 79–93.

Olsen, D. B., O. B. Brown, and S. R. Emmerson, 1983: Gulf Stream frontal statistics from Florida Straits to Cape Hatteras. *J. Geophys. Res.,* **88** (C8), 4569–4577.

Özgökmen, T. M., E. P. Chassignet, and A. M. Paiva, 1997: Impact of wind forcing, bottom topography and inertia on mid latitude jet separation in a quasi-geostrophic model. *J. Phys. Oceanogr.,* **27**, 2460–2476.

Parsons, A. T., 1969: A two-layer model of Gulf Stream separation. *J. Fluid Mech.,* **39,** 511–528.

Stern, M. E., 1997: Splitting of a free jet flowing over a saddle sill. *J. Geophys. Res.,* **102** (C9), 20 957–20 965.

——, and J. A. Whitehead, 1990: Separation of a boundary jet in a rotating fluid. *J. Fluid. Mech.,* **217,** 41–69.